Lec 3

(3·1)

The wilson's model for the Giant squid and the human and mammalian cortical neurons are given by

$$\cdot 8\,\dot{V} = -\left[17\cdot 81 + 47\cdot 71V + 32\cdot 63V^2\right](V - \cdot 55) - 26R(V + \cdot 92) + I$$

$$\dot{R} = \frac{1}{1\cdot 9}\left[-R + 1\cdot 35V + 1\cdot 03\right] \qquad (3\cdot 1)$$

Giant squid

where $100V$ is the voltage in millivolts.
$100I$ is the current in μA.

— x —

$$\dot{V} = -\left[17\cdot 81 + 47\cdot 58V + 33\cdot 8V^2\right](V - \cdot 48) - 26R(V + \cdot 95) + I$$

$$\dot{R} = \frac{1}{5\cdot 6}\left[-R + 1\cdot 29V + \cdot 79 + \cdot 33(V + \cdot 38)^2\right]$$

Human or Mammalian cortex

(3·2)

In this lecture we would like to study the bifurcation-diagram associated with these two models. But before we do so, let us study the FitzHugh Nagumo eqns once again.

3.1 FitzHugh Nagumo Equation

$$\dot{V} = 10\left[V - \frac{V^3}{3} - R + I_{input}\right] \tag{3·3}$$

$$\dot{R} = .8\left[-R + 1.25V + 1.5\right]$$

The equilibrium point of (3·3) is given by

$$\dot{V}=0 \Rightarrow R = V - \frac{V^3}{3} + I_{input}$$

$$\dot{R}=0 \Rightarrow R = 1{\cdot}25V + 1{\cdot}5 \qquad (3{\cdot}4)$$

For $V = V^*$, (3·4) can be solved as

$$R^* = 1{\cdot}25V^* + 1{\cdot}5 \qquad (3{\cdot}5)$$

$$I^*_{input} = 1{\cdot}25V^* + 1{\cdot}5 - V^* + \frac{V^{*3}}{3}$$

$$= \frac{1}{4}V^* + \frac{3}{2} + \frac{V^{*3}}{3} \qquad (3{\cdot}6)$$

We now claim that for any I^*_{input}, there is a unique real V^* that satisfies (3·6).

Proof of this claim

Multiply (3·6) by 3 we get

$$V^{*3} + \frac{3}{4} V^* + \left(\frac{g}{2} - I^*_{input}\right) = 0 \qquad (3\cdot 7)$$

Let $V^* = -\alpha$ be one real solution of (3·7). It would follow that the cubic polynomial in the l.h.s. of (3·7) would factor as

$$\left(V^* + \alpha\right)\left(V^{*2} - \alpha V^* + \left(\alpha^2 + \frac{3}{4}\right)\right) \qquad (3\cdot 8)$$

where $\alpha = \frac{g}{2} - I^*_{input}$.

Because

$$(-\alpha)^2 < 4\left(\alpha^2 + 3/4\right)$$

for any α, it follows that the

quadratic polynomial in (3·8) always factors with complex conjugate roots.

Thus (3·6) can be solved for a unique real V^* for any I_{inj}^*.

The conclusion is that for any I_{inj}, the FitzHugh Nagumo Eqns has a unique equilibrium V^*, R^* given by (3·5), (3·6).

Let us linearize (3·3) at the point of equilibrium (V^*, R^*) and obtain.

$$\dot{V} = \left(10 - \frac{10}{3} \cdot 3V^2\right)\Big|_{V=V^*} (V - V^*)$$

$$+ (-10)(R - R^*)$$

$$\dot{R} = 1(V - V^*) - \cdot 8(R - R^*)$$

Hence the Jacobian matrix $\bar{A}$ is given by

$$\bar{A} = \begin{pmatrix} 10 - 10V^{*2} & -10 \\ 1 & -\cdot 8 \end{pmatrix} \quad (3 \cdot 9)$$

3.7

$$\bar{A} = \begin{pmatrix} \theta & -10 \\ 1 & -.8 \end{pmatrix} \quad \text{where} \quad \theta = 10(1 - V^{*2})$$

Eigenvalues of $\bar{A}$ is given by

$$\begin{vmatrix} \lambda - \theta & 10 \\ -1 & \lambda + .8 \end{vmatrix} = \lambda^2 + (.8 - \theta)\lambda + 10$$

$$= \lambda^2 + (.8 - 10 + 10V^{*2})\lambda + 10$$

$$= \lambda^2 + (10V^{*2} - 9.2)\lambda + 10$$

$$\lambda = \frac{[9.2 - 10V^{*2}] \pm \sqrt{[9.2 - 10V^{*2}]^2 - 40}}{2}$$

Calculation Uno :

Find V^* when λ is always real.

$$\left[9.2 - 10V^{*2}\right]^2 = 40$$

$$\Rightarrow \left[9.2 - 10V^{*2}\right] = \pm\sqrt{40} = \pm 6.3245553$$

$$\Rightarrow 10V^{*2} = 9.2 \pm 6.3245553$$

$$\Rightarrow V^* = \pm 1.2459757, \pm .5362317$$

Calculation Duo :

Find V^* when λ is purely imaginary.

$$9.2 - 10V^{*2} = 0$$

$$\Rightarrow V^* = \pm .9591663.$$

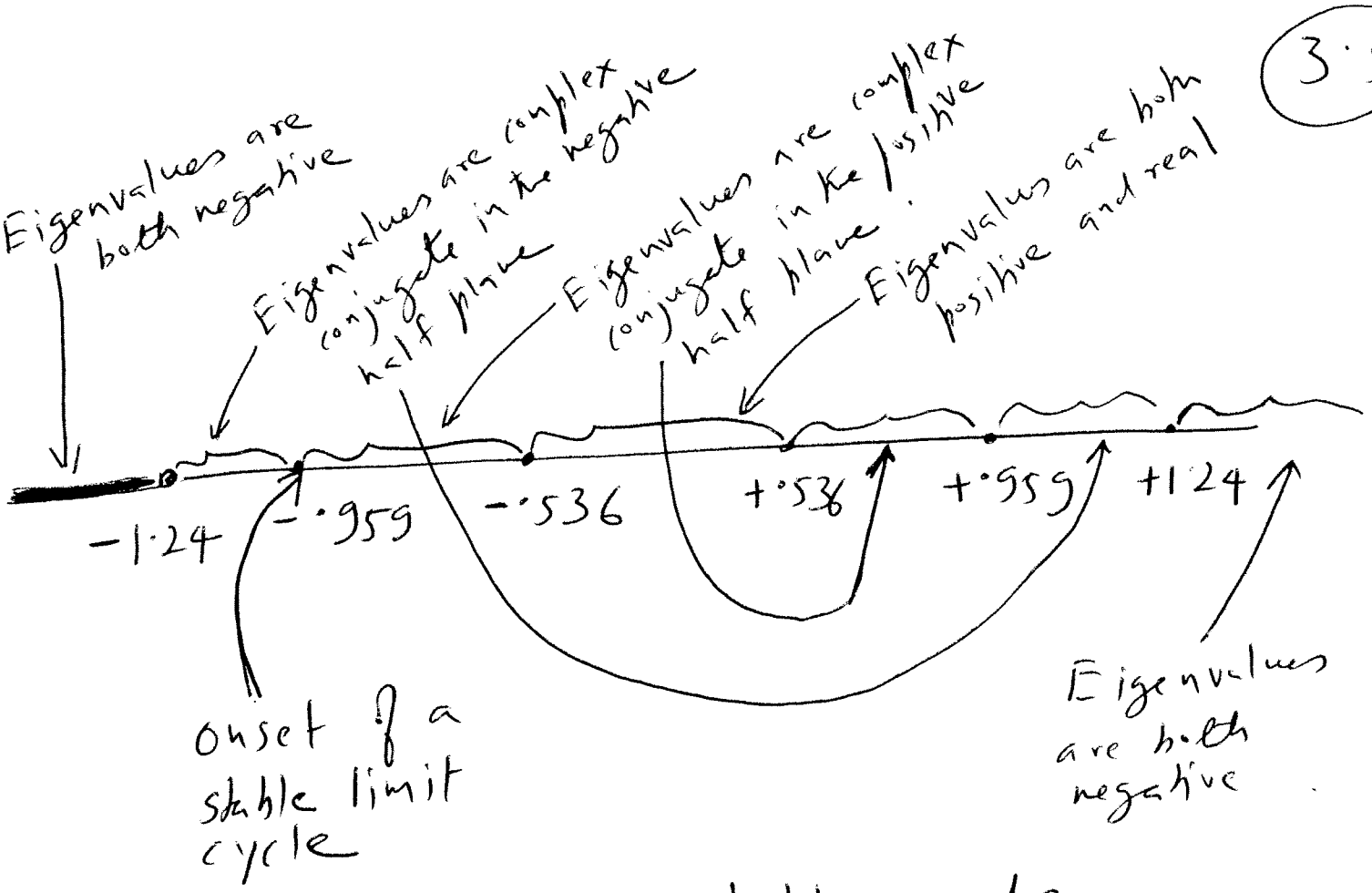

$|V^*| > 1.24$ stable node

$.959 < |V^*| < 1.24$ stable spiral point.

$.536 < |V^*| < .959$ unstable spiral point.

$0 \leq |V^*| < .536$ unstable node

When $V^* = -.959$ we have

$$I^*_{input} = -\frac{1}{4}(.959) + \frac{3}{2} - \frac{(.959)^3}{3}$$

$$= .9662586.$$

When $I_{input} = .9662586$, we have equilibrium at

$$V^* = -.959, \quad R^* = 2.69875$$

The linearized system has two eigenvalues at

$$\lambda = \pm i\, 3.1622773$$

For $I_{input} = .9662586$, the linearized eqn has a center at (V^*, R^*) and its soln oscillates with freq. $\omega = 3.1622773$.

For I_{input} slightly greater than $.9662586$, the linearized system is an unstable spiral and the non-linear system has a stable limit cycle.

3·12

$$R = V - \frac{V^3}{3} + \cdot 9662586 .$$

$$R = 1 \cdot 25V + 1 \cdot 5$$

Point 2 is $(-3, 6 \cdot 9662586)$

$$R = -3 + \frac{27}{3} + \cdot 9662586 .$$

$$= 6 \cdot 9662586 .$$

Point 1 is $(4 \cdot 3730069, 6 \cdot 9662586)$

3.13

Point 3 is

$$(-3, -2.25)$$

Point 4 is $(4.3730069, -2.25)$

$\dot{V}$ on point 4 is

$$10\left(4.3730069 - \frac{(4.3730069)^3}{3} + 2.25 + .9662586\right)$$

$$10\,(7.5892655 - 27.87528)$$

$$= -202.86$$

$\therefore \dot{V} < 0$ at point 4, the point 4 is located to the right of the isocline $\dot{V} = 0$.

3.14

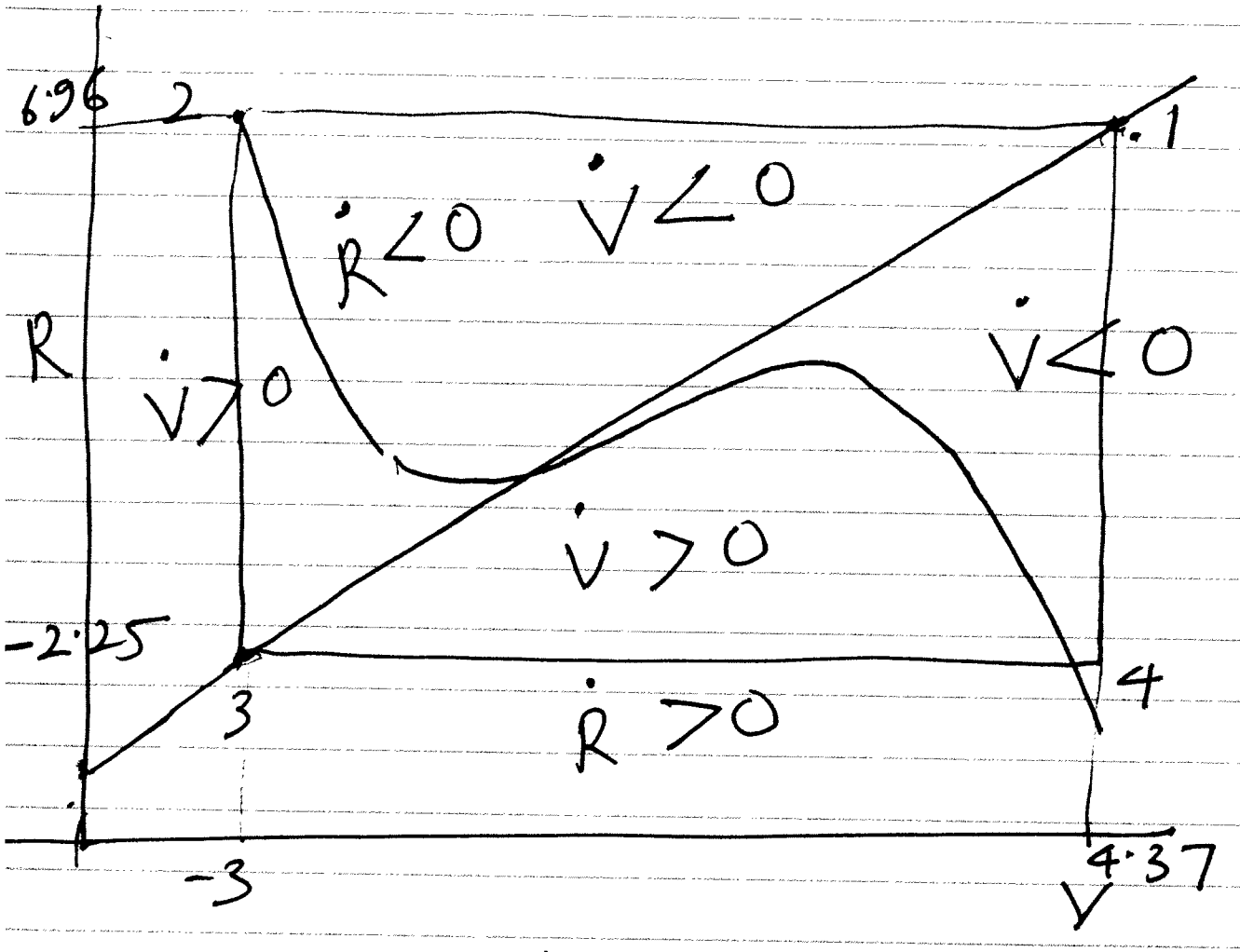

The vector field (3.3) assuming $I_{input} = .9662586$ always points inwards on the boundary of the rectangle with corners at points ①, ②, ③, ④.

3.15

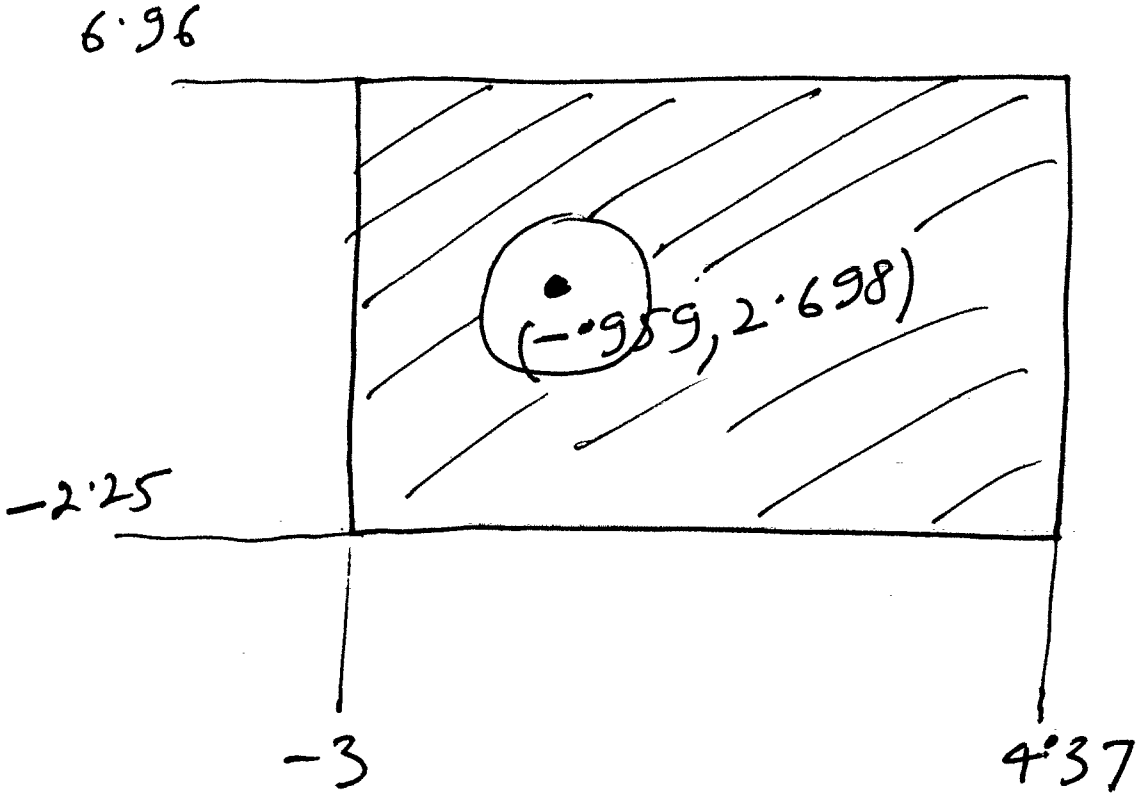

In this annular region, the vector field always points inwards. Hence by poincare-Bendixon theorem there is at least one stable limit cycle.

Conclusion:

We have shown that for the FitzHugh Nagumo Eqn (3.3), when I_{input} exceeds the value .9662586 slightly, the linearized dynamics crosses from a stable equilibrium to an unstable spiral. The nonlinear equation has atleast one stable limit cycle, a fact we conclude from the Poincare-Bendixon theorem.

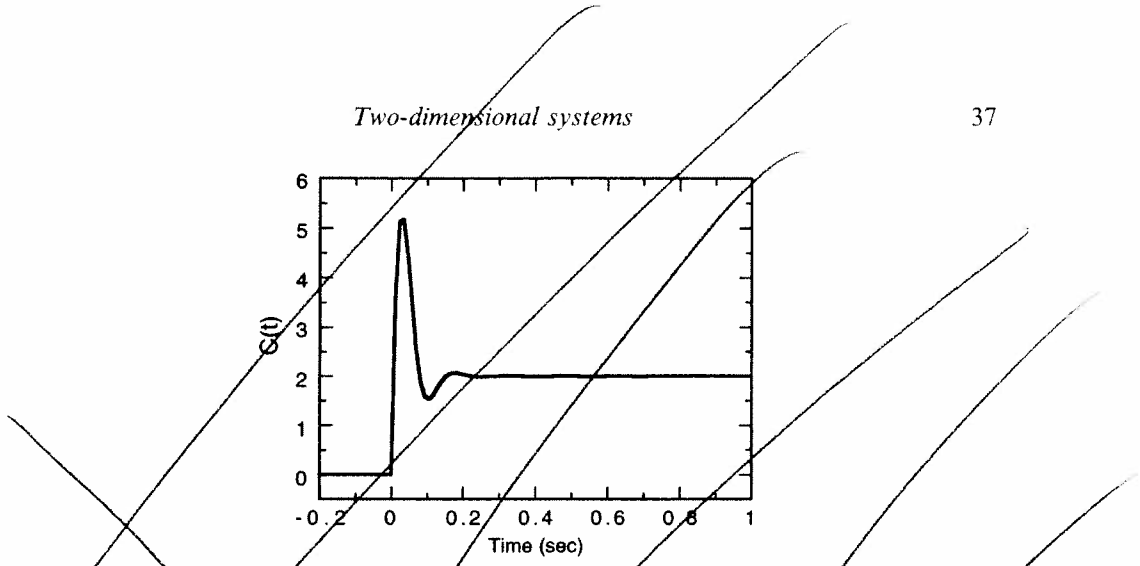

Fig. 3.2 Solution $C(t)$ to (3.21) as represented by (3.24). The response at stimulus onset ($t = 0$) is very similar to that of the primate cone in Fig. 3.1.

The equilibrium values (2, 2) have been added in accord with Theorem 2. $C(t)$ is plotted as a function of time in Fig. 3.2. The similarity between the solution (3.24) and the physiological data in Fig. 3.1 is apparent. The response at the termination of light stimulation has not been plotted in Fig. 3.2, but it is mathematically the mirror image of the response to stimulus onset, and this is evident from the experimental data.

3.4 Stability and state space

Based on Theorem 2, all possible solutions of second order differential equations with constant coefficients may now be grouped into a small number of categories. This categorization is based on the fact that the characteristic equation is quadratic and therefore must have exactly two roots. We have already seen that the unique equilibrium point for a linear differential equation can always be translated to the origin. Thus, it might be expected that solutions can be characterized by their behavior near the origin. An important concept here is that of a trajectory. A **trajectory** is the entire time course of the solution of a differential equation from $t = 0$ to $t = \infty$, given a particular initial condition. Thus, any differential equation defines an infinite number of trajectories, each corresponding to a different initial condition. Additionally, note that an equilibrium point is itself a trajectory, since a trajectory starting at equilibrium must by definition remain there for all eternity!

We may now define the concepts of stability, asymptotic stability, and instability of an equilibrium point. An equilibrium point of a system of differential equations is **asymptotically stable** if all trajectories starting within a region containing the equilibrium point decay to that point exponentially as $t \to \infty$. Conversely, the equilibrium is **unstable** if at least one trajectory beginning in a region containing the point leaves that region permanently. Finally, an equilibrium is **stable** or **neutrally stable** if nearby trajectories remain nearby as $t \to \infty$ but do not approach asymptotically.

Trajectories for second order differential equations may be conveniently plotted in a two-dimensional space in which the variables of the equations define the axes. Such a space is known as a **state space** or a **phase space**, terms that will be used interchangeably. Analytical solution of the system equations yields explicit functions of t, such as $C(t)$ and $H(t)$ in (3.24). If time is regarded as a parameter, then it is possible to plot the entire course of each system trajectory as a curve in the phase space. Phase space plots reveal the relationship between the variables at all points on the trajectory. Both the time dependence of solutions and the phase space are plotted by **LinearOrder2.m**, and experimentation with that program will provide a great deal of insight into the nature of phase space trajectories. Note that the phase space plot contains arrows indicating the local directions in which trajectories flow at various points in the space.

All possible solutions to the second order differential equation described in Theorem 2 may now be categorized and their phase space trajectories illustrated. From the fact that the characteristic equation is quadratic with real coefficients, the two eigenvalues must either both be real, both be pure imaginary, or else be a complex conjugate pair. The possibilities are enumerated below, and typical equations are given along with solutions for initial conditions $x(0) = 1, y(0) = 1$.

A **spiral point** results when the eigenvalues are a complex conjugate pair. Thus, the solutions are in the form of exponentials multiplied by a sine and a cosine. The spiral point is asymptotically stable if the real part of the eigenvalues is negative. A typical trajectory of an asymptotically stable spiral point is plotted in the upper left of Fig. 3.3, which makes

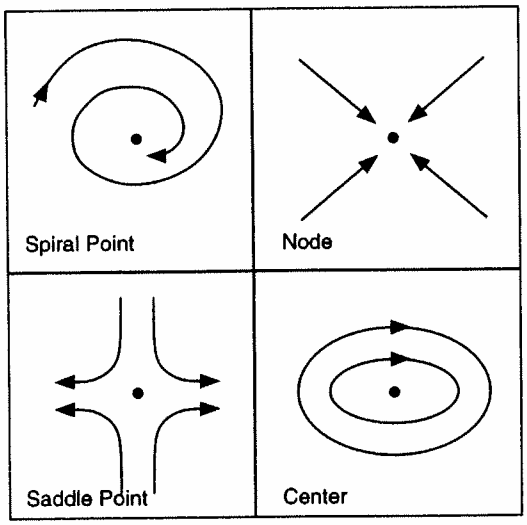

Fig. 3.3 Typical phase plane trajectories for the four characteristic equilibrium points of linear dynamical systems: spiral point, node, saddle point, and center. The horizontal and vertical axes represent the two variables describing each system. Equilibrium points are depicted by a dot in the center of each plot. Trajectories illustrated for the spiral point and node are asymptotically stable. Saddle points are always unstable, while centers are stable but not asymptotically stable.

clear that the trajectory is in fact a spiral. The following equation provides an example of a system with an asymptotically stable spiral point:

$$\frac{\mathrm{d}}{\mathrm{d}t}\begin{pmatrix}x\\y\end{pmatrix} = \begin{pmatrix}-2 & -16\\ 4 & -2\end{pmatrix}\begin{pmatrix}x\\y\end{pmatrix}$$

solution :

$$x(t) = \mathrm{e}^{-2t}\cos(8t) - 2\,\mathrm{e}^{-2t}\sin(8t) \tag{3.25}$$
$$y(t) = \mathrm{e}^{-2t}\cos(8t) + 0.5\,\mathrm{e}^{-2t}\sin(8t)$$

The equilibrium point is a **node** if the eigenvalues are both real and have the same sign. The node is asymptotically stable if the eigenvalues are negative, and it is unstable if they are positive. Typical trajectories at a node are plotted in Fig. 3.3, and an illustrative example is:

$$\frac{\mathrm{d}}{\mathrm{d}t}\begin{pmatrix}x\\y\end{pmatrix} = \begin{pmatrix}-2 & 4\\ 0 & -3\end{pmatrix}\begin{pmatrix}x\\y\end{pmatrix}$$

solution :

$$x(t) = 5\,\mathrm{e}^{-2t} - 4\,\mathrm{e}^{-3t} \tag{3.26}$$
$$y(t) = \mathrm{e}^{-3t}$$

A **saddle point** occurs when both eigenvalues are real but have opposite signs. Because one eigenvalue is positive, all saddle points are unstable. As illustrated in Fig. 3.3, trajectories approach a saddle point along one axis (y in this example) but diverge from it along a different axis (x in this case). Typical equations generating a saddle point are:

$$\frac{\mathrm{d}}{\mathrm{d}t}\begin{pmatrix}x\\y\end{pmatrix} = \begin{pmatrix}2 & -1\\ 0 & -3\end{pmatrix}\begin{pmatrix}x\\y\end{pmatrix}$$

solution :

$$x(t) = 0.8\,\mathrm{e}^{2t} + 0.2\,\mathrm{e}^{-3t} \tag{3.27}$$
$$y(t) = \mathrm{e}^{-3t}$$

The final possibility is that the pair of eigenvalues are pure imaginary, and this condition defines a **center**. Euler's formula (1.15) in this case dictates that all trajectories must be a sum of a sine and a cosine of the same frequency. Because of this, all trajectories around a center will be strictly periodic oscillations. Because any periodic function repeats itself, phase space trajectories around a center will always be closed circular or ellipsoidal

conveniently plotted in a
ıs define the axes. Such a
l be used interchangeably.
tions of t, such as $C(t)$ and
ɔossible to plot the entire
. Phase space plots reveal
rajectory. Both the time
by **LinearOrder2.m**, and
insight into the nature of
ins arrows indicating the
he space.
n described in Theorem 2
rated. From the fact that
he two eigenvalues must
ɔlex conjugate pair. The
ven along with solutions

ɔnjugate pair. Thus, the
a cosine. The spiral point
tive. A typical trajectory
of Fig. 3.3, which makes

points of linear dynamical
:al axes represent the two
ı the center of each plot.
Saddle points are always

shapes like those plotted in the lower right of Fig. 3.3. A typical example of a system with a center is:

$$\frac{\mathrm{d}}{\mathrm{d}t}\begin{pmatrix} x \\ y \end{pmatrix} = \begin{pmatrix} 1 & -2 \\ 5 & -1 \end{pmatrix}\begin{pmatrix} x \\ y \end{pmatrix} \tag{3.28}$$

solution :

$$x(t) = \cos(3t) - 0.33\sin(3t)$$
$$y(t) = \cos(3t) + 1.33\sin(3t)$$

As the nature of the solutions and their stability are determined by the eigenvalues of the characteristic equation, all trajectories for all possible initial conditions will have the same qualitative behavior in any given linear system. However, this holds true only for linear systems, and it must be qualified when nonlinear systems are discussed. Indeed, the power and elegance of phase space representations can only be fully appreciated in nonlinear dynamics.

3.5 Critical damping and muscle contraction

Theorem 2 covers all possible second order linear differential equations except for one: the case where both roots of the characteristic equation are identical. The case of two identical roots is generally called **critical damping** for historical reasons deriving from physics. Critical damping is an exceptional case, as the probability that the coefficients of the characteristic equation, if chosen at random, would generate identical eigenvalues is zero. Nevertheless, it is easy to construct mathematical examples in which the two eigenvalues are identical, and these will be solved now. Physiologically, critical damping is significant because it represents the simplest approximation to the dynamics of muscle contraction. In addition, the cascades of equations treated in the previous chapter are another case of critical damping (because the time constants of all stages are identical).

Let us motivate critical damping by considering a simple model of muscle contraction. Figure 3.4 plots data on the force generated by a cat soleus muscle as a function of length at two different levels of motorneuron activation (Rack and Westbury, 1969). Although the overall curves are nonlinear, above an equilibrium length, x_0, the force generated is nearly linear over the considerable range indicated by the solid lines. No force is generated for $x < x_0$, a state where the muscle is relaxed. The equilibrium length shifts to smaller values as the level of motorneuron activity increases. Neural specification of x_0 is believed to be the way in which the central nervous system determines the desired length and force exerted by each muscle in the body, and this is termed the 'equilibrium point hypothesis'. Over the linear range, the force of contraction is of the form $\alpha^2(x - x_0)$, where the length of the muscle x is always assumed to be greater than or equal to x_0. The force of contraction is generated as actin–myosin bonds are formed, after which a configurational change in the myosin head causes the muscle fiber to shorten (see Rothwell, 1994). There is also some frictional resistance to contraction within the muscle due to the

Fig. 3.4 Force generated
permission, Rack and We
portion (solid lines) of t
equilibrium length at whi

breaking of actin–my
the velocity of contr
traction leads to the e

It is easy to see that th
defining the new vari
chosen so that the res
will have identical eige

so $\lambda = -\alpha$. This is t
Theorem 2. One soluti

where a is determined
solution, just as there a
Whatever form the se
Let us therefore guess
second solution of the f

8 *Nonlinear oscillations*

The study of nonlinear dynamical systems in the last two chapters has enabled us to analyze rather complex neural networks in terms of the stability of their equilibrium states. However, we have yet to consider one of the most exciting and important topics in all of dynamical systems theory: nonlinear oscillations. Indeed, nonlinear oscillations, or rhythms, are ubiquitous in living organisms. Circadian rhythms, cardiac rhythms, hormonal cycles, the rhythms of breathing and locomotion (walking, running, swimming): all are of the essence of life. Not only are many of these rhythms generated by neural networks, but we shall shortly see that even the generation of action potentials in single neurons is the result of inherently nonlinear oscillations.

In linear systems the only possible oscillations involve sines and cosines. These linear oscillations form closed circular or elliptical trajectories around an equilibrium point that is a center. Furthermore, if the initial conditions are changed even slightly, the result is a neighboring oscillatory solution with the same form in the phase plane but a different amplitude. No other type of oscillation is possible in a linear system, regardless of whether it has two or two thousand dimensions. In the nervous system and other biological systems, there is always some degree of noise resulting from physiological or environmental fluctuations. Such noise would continuously alter the amplitude of a linear oscillation, causing it to wander around the state space rather aimlessly. Clearly, such a sloppy linear oscillation could not control one's breathing or heartbeat very effectively. As we shall see, nonlinear oscillations are largely immune to this noise problem. For this reason alone, it is safe to conclude that biological rhythms evolved to be inherently nonlinear. To even begin to understand the rhythms of life and the nervous system, it is thus essential to study nonlinear oscillations.

8.1 Limit cycles

Let us start discussion of nonlinear oscillations with the definition of an oscillation itself. A trajectory $X(t)$ of a dynamical system with any number of dimensions is an **oscillation** if:

$$\vec{X}(T+t) = \vec{X}(t) \quad \text{for some unique } T > 0 \text{ and all } t. \tag{8.1}$$

This states that the system will always return to exactly the same state after time T, and T is therefore called the **period** of the oscillation. Note that if (8.1) is true for T, it will also be true for NT where N is any integer > 0, so the period is defined to be the minimum T for which (8.1) is holds. Also, the requirement that T be unique excludes equilibrium points,

(8.1) would otherv
ıtion. Note that (8.
ear system is perio
hborhood of a give
oscillation of any amplitud
determined by the initial cc
oscillations, but this is rare ir
that nonlinear systems can g
non-oscillatory trajectories t
over time. Let us make this p

Definition: An **oscillatory**
limit cycle if all trajectori
are spirals. If these neig
$t \to \infty$, then the limit cy
trajectories spiral away fr

Figure 8.1 shows schematic il
cycles in the phase plane of a t
cycle only requires that traject
for this restriction is that mar
from one another.

Before exploring limit cycl
analytical tools to predict the
dimensional systems, as the
intuitive in this case. A very
cycles, states that a limit cycle

Theorem 9: If a limit cycle
must necessarily surround
that one must be a node,
surrounds more than one e
satisfied:

where N is the number of (n
saddle points.

The requirement that the syst
constant. This guarantees that
differential equations describin

for which (8.1) would otherwise hold. The reciprocal of T, $1/T$, is termed the **frequency** of the oscillation. Note that (8.1) applies to linear systems as well as nonlinear.

If a linear system is periodic, there are infinitely many periodic solutions within any small neighborhood of a given oscillation: as the solution is a sum of sines and cosines, an oscillation of any amplitude whatsoever is a solution. (The amplitude is, of course, determined by the initial conditions.) Nonlinear systems can also produce analogous oscillations, but this is rare in biological systems. Of vastly greater significance is the fact that nonlinear systems can generate isolated oscillations that are surrounded by open, non-oscillatory trajectories that either spiral towards or else away from the oscillation over time. Let us make this precise with a definition:

> **Definition**: An **oscillatory** trajectory in the state space of a nonlinear system is a **limit cycle** if all trajectories in a sufficiently small region enclosing the trajectory are spirals. If these neighboring trajectories spiral towards the limit cycle as $t \to \infty$, then the limit cycle is **asymptotically stable**. If, however, neighboring trajectories spiral away from the limit cycle as $t \to \infty$, the limit cycle is **unstable**.

Figure 8.1 shows schematic illustrations of both asymptotically stable and unstable limit cycles in the phase plane of a two-dimensional system. Notice that the definition of a limit cycle only requires that trajectories which are sufficiently close be open spirals. The reason for this restriction is that many nonlinear systems contain several limit cycles separated from one another.

Before exploring limit cycles in neuroscience, it will be necessary to develop some analytical tools to predict their existence. Let us first restrict our consideration to two-dimensional systems, as the relevant theorems are both more numerous and more intuitive in this case. A very useful theorem due to Poincaré, the discoverer of limit cycles, states that a limit cycle must surround one or more equilibrium points:

> **Theorem 9**: If a limit cycle exists in an autonomous two-dimensional system, it must necessarily surround at least one equilibrium point. If it encloses only one, that one must be a node, spiral point, or center, but not a saddle point. If it surrounds more than one equilibrium point, then the following equation must be satisfied:
>
> $$N - S = 1$$
>
> where N is the number of (nodes + spiral points + centers), and S is the number of saddle points.

The requirement that the system be autonomous means that all coefficients must be constant. This guarantees that no trajectory can cross itself. The reason is simple: the differential equations describing the system define a unique direction at every point in

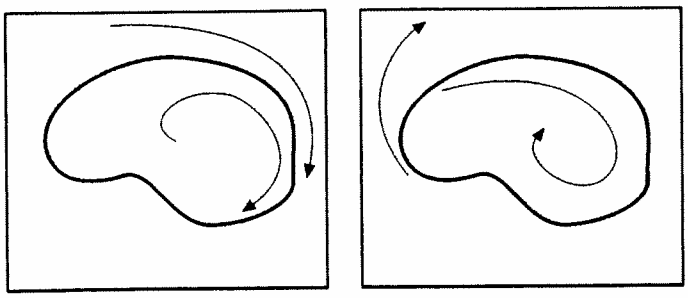

Fig. 8.1 Closed curves depict an asymptotically stable limit cycle (left) and an unstable limit cycle (right). Neighboring trajectories are plotted by arrows.

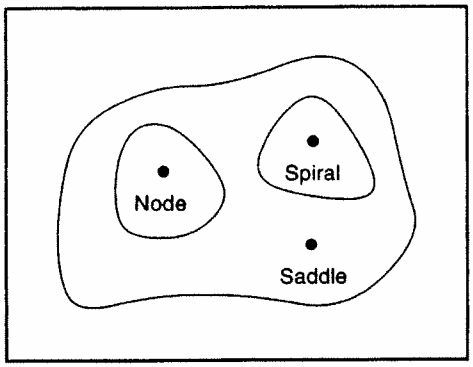

Fig. 8.2 Phase plane of a two-dimensional dynamical system with the three steady states indicated. Theorem 9 indicates that any possible limit cycle must surround one of the sets of steady states indicated by the three closed curves.

state space. If a trajectory were to cross itself, there would have to be two different directions specified by the equations at some point, but this is impossible unless the coefficients of the equations change with time, which has been prohibited. An intuitive grasp of Theorem 9 can therefore be gained from the observation that trajectories originating inside a limit cycle in the phase plane can never cross the limit cycle because it is a closed oscillatory trajectory. Therefore, these trajectories must either originate or terminate somewhere, and that must be a steady state (or another limit cycle which itself surrounds a steady state, etc.)

Figure 8.2 illustrates the possible locations for limit cycles in a two-dimensional system with three steady states: a node, a spiral point, and a saddle point. In this example, Theorem 9 precludes a limit cycle around any pair of the steady states. Note that Theorem 9 tells us nothing about the exact location or size or even the existence of the limit cycle but only about the set of steady states it would have to enclose if it existed.

Theorem 9 is a necessary but by no means sufficient condition for the existence of limit cycles in a nonlinear system. In Chapter 6, for example, we encountered several nonlinear systems with multiple steady states, such as two nodes and a saddle point, and yet there

were no limit cycles to be
conditions under which
exists for two-dimensiona
then sketch a proof using

Theorem 10 (Poincar
autonomous (i.e. cons
conditions: (1) the ann
that cross the boundar
at least one asymptoti

Theorem 10 is easily ur
region (gray) that satisfies
the annulus must surroun
however, that this steady
the annular region itself, s
Fig. 8.3 show representati
boundaries as required b
conditions of the theorem
to rest, because there are n
is autonomous, no two en
entering from region A anc
one closed trajectory that
asymptotically stable limit
proof of the Poincaré–Ben

It is important to recogn
least one asymptotically sta
number of limit cycles. In
asymptotically stable, beca

Fig. 8.3 Annulus (gray region) f
(unstable), and trajectories enter t
within the annulus.

were no limit cycles to be found in those cases. What we need is a theorem that specifies conditions under which a system must have a limit cycle. Fortunately, such a theorem exists for two-dimensional systems. Let us first state the **Poincaré–Bendixon Theorem** and then sketch a proof using diagrams.

> **Theorem 10 (Poincaré–Bendixon)**: Suppose there is an annular region in an autonomous (i.e. constant coefficient) two-dimensional system that satisfies two conditions: (1) the annulus contains no equilibrium points; and (2) all trajectories that cross the boundaries of that annulus enter it. Then the annulus must contain at least one asymptotically stable limit cycle.

Theorem 10 is easily understood by examining Fig. 8.3. This figure shows an annular region (gray) that satisfies the conditions of the theorem. To be consistent with Theorem 9, the annulus must surround a node, spiral point, or center, which is plotted as a dot. Note, however, that this steady state, although surrounded by the annulus, is not within the annular region itself, so it does not violate the conditions of the theorem. Arrows in Fig. 8.3 show representative trajectories entering the annulus over both its inner and outer boundaries as required by Theorem 10. Once these trajectories enter the annulus, the conditions of the theorem guarantee that they can never leave. Also, they can never come to rest, because there are no equilibrium points in the annulus. Finally, because the system is autonomous, no two entering trajectories can ever cross one another. As trajectories entering from region A and region B move closer together, therefore, there must be at least one closed trajectory that they approach asymptotically. Thus, there must be at least one asymptotically stable limit cycle enclosed within the annulus. This completes an intuitive proof of the Poincaré–Bendixon theorem.

It is important to recognize that Theorem 10 specifies that the annulus must contain at least one asymptotically stable limit cycle, but the theorem also permits there to be an odd number of limit cycles. In this case, the outer and inner limit cycles would have to be asymptotically stable, because trajectories entering the annulus across the outer and inner

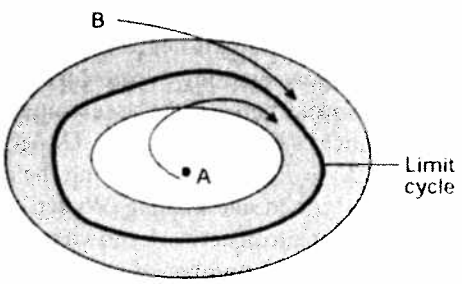

Fig. 8.3 Annulus (gray region) fulfilling the requirements of Theorem 10. Region A contains a steady state (unstable), and trajectories enter the annulus from both regions A and B. As indicated, a limit cycle must exist within the annulus.

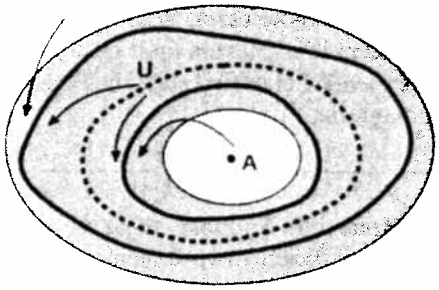

Fig. 8.4 Schematic of an annulus (gray region) satisfying Theorem 10 but containing three limit cycles. Two are asymptotically stable (solid curves), but the intervening one (dashed curve) must be unstable. A is an unstable node or spiral point. Representative trajectory directions are shown by the arrows.

boundaries must all approach limit cycles (not necessarily the same one). If there is more than one limit cycle, asymptotically stable limit cycles must alternate with unstable limit cycles. You can convince yourself of this by imagining what would happen to trajectories originating between two nested, asymptotically stable limit cycles: they would have to be separated by an unstable limit cycle, which is illustrated schematically in Fig. 8.4. Although the existence of alternate asymptotically stable and unstable limit cycles may seem to be an unlikely occurrence, they are actually predicted by the Hodgkin–Huxley equations, and their existence has been experimentally verified! Armed with Theorems 9 and 10, we are now ready to study limit cycles in two-dimensional neural systems.

8.2 Wilson–Cowan network oscillator

As a first application of these criteria to neural oscillations, let us consider a localized (i.e. non-spatial) version of the Wilson–Cowan (1972) equations. The equations presented here are the simplest example of these equations that possesses a limit cycle. Consider a four-neuron network consisting of three mutually excitatory E neurons which in turn stimulate one inhibitory I neuron that provides negative feedback onto the three E cells as depicted on the left in Fig. 8.5. Neural circuits like this are typical of the cortex, where inhibitory GABA neurons comprise about 25% of the total population of cortical cells with the rest being mainly excitatory glutamate neurons (Jones, 1995). Thus, the network in Fig. 8.5 may be thought of as approximating a local cortical circuit module.

Let us simplify the Wilson–Cowan network by assuming that all E neurons receive identical stimuli and have identical synaptic strengths. Under these conditions we can invoke symmetry and set $E_1 = E_2 = E_3$, thereby reducing the number of neurons in the network, a procedure sometimes termed **subsampling** (Wallén *et al.*, 1992). This results in the mathematically equivalent two-neuron network shown on the right in Fig. 8.5. In fact, we can generalize this argument to any number of mutually excitatory and inhibitory neurons with identical interconnections, so the key concept is that of recurrent excitation coupled with recurrent inhibition. Note that by reducing the network to two neurons (or two neural populations), the recurrent excitation is transformed into equivalent

is subthreshold, as no action potentials are generated. Comparing Fig. 8.8 with responses from the Hodgkin–Huxley equations depicted in Fig. 9.1 and 9.3 of the next chapter shows that (8.8) does not provide a very accurate description of action potential shapes. Nevertheless, the FitzHugh–Nagumo equations provide mathematical insight into the nature of neuronal excitability, namely that spikes are generated when I_{input} becomes strong enough to destabilize the equilibrium state (see Exercises).

8.4 Hopf bifurcations

Theorems 9 and 10 provide us with powerful means to determine whether limit cycles exist in a nonlinear system. Unfortunately, however, both theorems are limited to two-dimensional systems and do not apply when more than two neurons or two ion flows are involved. Theorem 9 does not generalize to higher dimensions, because a closed trajectory defining a limit cycle oscillation cannot be said to enclose equilibrium points in three or more dimensions in any meaningful sense. One might think at first that the Poincaré–Bendixon theorem (Theorem 10) would generalize to higher dimensions if instead of specifying an annulus into which trajectories flow, one specified a solid 'doughnut' shape in three dimensions or a 'hyper-doughnut' in higher dimensional systems. However, such a ploy also fails to guarantee the existence of a limit cycle, because trajectories need not be closed to avoid crossing in higher dimensions. This means that a trajectory might remain within the doughnut but be chaotic (see Chapter 11) rather than being a limit cycle oscillation. Fortunately, there is one powerful theorem that applies to a system with any number of dimensions from two up, the Hopf bifurcation theorem.

Theorem 11 (Hopf bifurcation theorem): Consider a nonlinear dynamical system in $N \geq 2$ dimensions that depends on a parameter β:

$$\frac{d\vec{X}}{dt} = \vec{F}(\vec{X},\beta)$$

Let X_0 be an isolated equilibrium point of this system. Assume that there is a critical value $\beta = \alpha$ with the following properties determined from the Jacobian, $A(\beta)$: (1) X_0 is asymptotically stable for some finite range of values $\beta < \alpha$. (2) When $\beta = \alpha$ the system has one pair of pure imaginary eigenvalues $\lambda = \pm i\omega$ while all other eigenvalues have negative real parts. (3) X_0 is unstable for some range of values $\beta > \alpha$. Then either the system possesses an asymptotically stable limit cycle over a range $\beta > \alpha$ or else it possesses an unstable limit cycle over some range $\beta < \alpha$. Near $\beta = \alpha$ the frequency of this oscillation will be approximately $\omega/2\pi$, and the oscillation will emerge with infinitesimal amplitude sufficiently close to α.

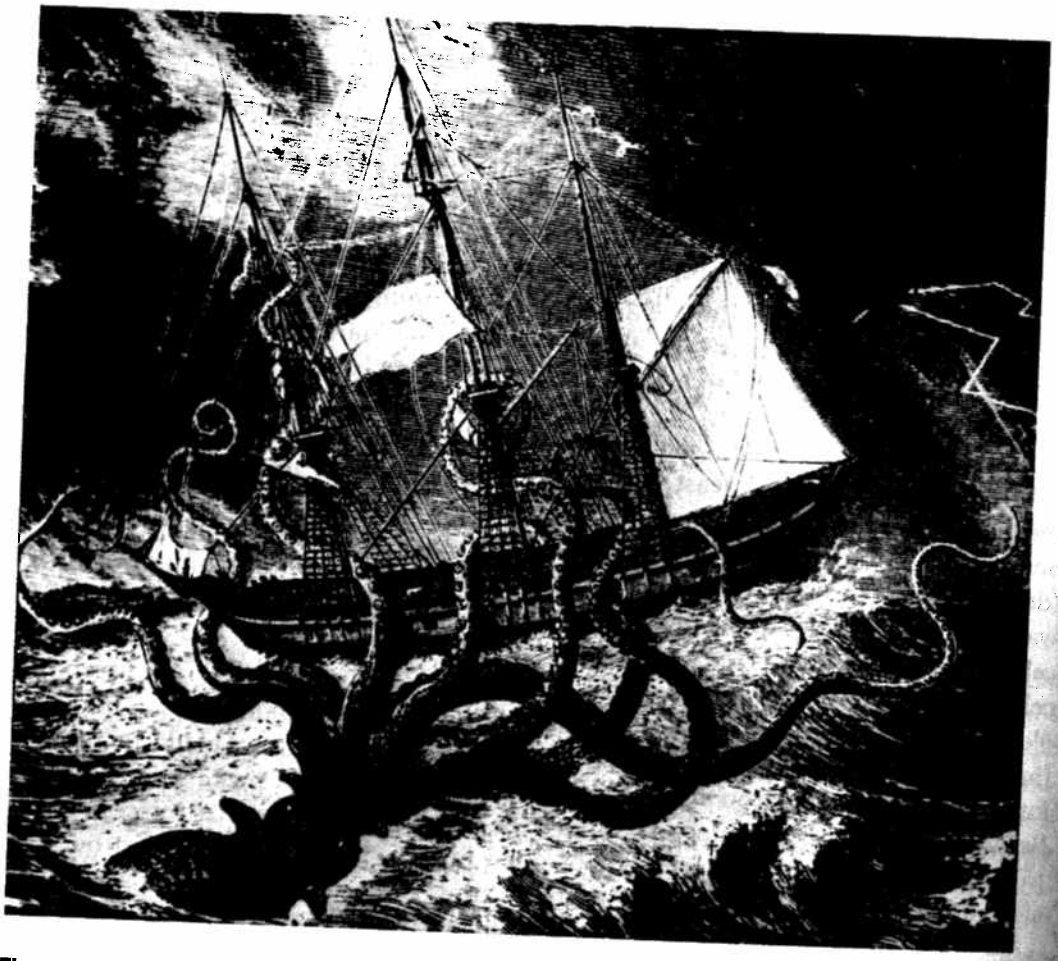

Figure 4.1 The infamous giant squid, having nothing to do with the work of Hodgkin and Huxley on squid giant axon. From *Dangerous Sea Creatures*, © 1976, 1977 Time-Life Films, Inc.